Title
Geotechnical centrifuge modelling of thermal improvement processes in clayey soils for offshore anchoring purposes

Authors
de Souza Ferreira, Marina
Saboya, Fernando
Tibana, Sérgio
et al.

Publication Date
2025-04-01

DOI
10.1016/j.oceaneng.2025.120550

GEOTECHNICAL CENTRIFUGE MODELLING OF THERMAL IMPROVEMENT PROCESSES IN CLAYEY SOILS FOR OFFSHORE ANCHORING PURPOSES

Marina de Souza Ferreira
Alta Engenharia, Rio de Janeiro, Brazil, marinadesferreira@gmail.com

Fernando Saboya Jr., Sérgio Tibana, Rodrigo Martins Reis
State University of Norte Fluminense - Uenf, Campos, RJ, Brazil, saboya@uenf.br , tibana@uenf.br, reis@uenf.br

John Scott McCartney
Professor- University of California San Diego, Department of Structural Engineering, j1mccartney@ucsd.edu

Ricardo Garske Borges
Petrobras, Rio de Janeiro, Brazil, garske@petrobras.com.br

Anchoring designs for offshore platforms are a constant challenge for geotechnical engineers, particularly when the seabed soil has unfavorable shear strength and deformation characteristics. This has prompted the search for innovative soil improvement techniques. This study involves geotechnical centrifuge modelling of thermal consolidation in lightly overconsolidated clayey soil by heating a torpedo pile (anchor) to improve the soil's mechanical response and torpedo pile pullout capacity. The centrifuge tests evaluated the improvement in soil shear strength after thermal consolidation under two different temperatures (45 and 65°C) and subsequent cooling via T-bar penetration tests during centrifuge testing. Undrained shear strength in these tests was 1.5 to 3 times higher than that of untreated soil. This increase was found to be dependent on the maximum temperature reached at a given location in the soil. This study demonstrates that thermal improvement is a feasible and efficient technical alternative to improve soils in offshore settings since classic soil improvements solutions developed for onshore conditions cannot be applied in deep- or ultradeep-water.

INTRODUCTION

The discovery of deep and ultradeep water oil and gas fields prompted the oil and gas industry to seek solutions that would enable these environments to be fully exploited. These physical conditions required a shift from fixed to floating platforms, which called for solutions that would guarantee the positioning and stability of drilling platforms on the ocean surface (Lauria et al., 2024, Han & Liu, 2020, Raaj et al., 2023).

In recent decades, different anchor designs and arrangements have been used to securely position floating platforms, including vertical load anchors (VLAs) and suction and torpedo piles, used in catenary or taut leg mooring systems (Rui et al., 2024). The fundamental difference between these two systems is that catenary mooring systems apply predominantly horizontal forces to the anchor, whereas the taut leg system applies both horizontal and vertical forces to the anchor as the angle between the mooring lines and seabed is approximately 45°. These arrangements can result in extremely large mooring areas, especially at water depths of thousands of meters. Large mooring areas can limit the exploitation of the offshore deposit due to the large spacing between platforms.

Another factor in the complexity of platform positioning is the low bearing capacity of the soil generally found on the seabed. The geotechnical profile of clayey seabed typical of the Brazilian coastline suggests that the first few meters, where anchors are naturally installed, consists of slightly overconsolidated fine-grained soil with low shear strength and insufficient anchor pullout capacity. To meet the mechanical performance requirements of mooring systems, solutions to date have been limited to increasing the number of anchors per platform or increasing the anchor size. The first solution results in an undesirable and inconvenient increase in the number of mooring lines, while the second raises the costs of transporting and installing anchors, and both having a considerable impact on logistics.

Improving the shear strength of clayey soil layers is a widely studied topic in the geotechnical community. Different techniques are investigated in the literature, such as incorporating rigid structures, placement of surficial embankments for overconsolidation, chemical treatment, vacuum consolidation, and electroosmosis, among others. However, these techniques require easy access to the soil surface. In mooring systems with water depths of hundreds to thousands of meters, conventional alternatives for soil improvement are not feasible. Improvement of the shear strength of the seabed soil will result in fewer anchors that can be moored vertically, reducing the size of the surrounding area. One strategy that may be technically feasible is thermal consolidation of the soil using the anchor itself as a heat source, thus improving the mechanical response of the soil in the area around the anchors. This approach has been investigated in a limited number of tests on torpedo anchors by Ghaaowd et al., (2022), but further testing is necessary to understand the zone of influence of thermal consolidation around the anchor.

In this respect, an experimental study was conducted using centrifuge-scale physical models to assess the efficiency of thermal consolidation in improving the shear strength properties of marine clay layers. A cylindrical heat source was fabricated with geometry similar to that of a torpedo pile, and the physical model of the soil layer was instrumented with pore pressure transducers and thermocouples at different locations from the heat source. The undrained shear strength profiles were obtained via T-bar testing during the centrifuge run, before and after thermal consolidation.

BACKGROUND

Campanella and Mitchell (1968) observed different behavior between normally consolidated (NC), lightly (LOC) and heavily overconsolidated (OC) clayey soil after a heating and cooling cycle, with volumetric contraction in LOC or NC and moderate expansion in OC. Abuel-Naga et al. (2007) and Ghaaowd et al. (2015) also reported that pore water pressure due to heating and post-cooling deformation are dependent on soil stress history. After a soil heating and cooling cycle, Campanella and Mitchell (1968), Trani et al. (2008) and Abuel-Naga et al. (2007) reported a return to initial pore water pressure in NC clays and negative final pore water pressure in OC clays. Pore water pressures are only observed during undrained heating, which will dissipate after time if drainage is permitted.

Researchers such as Houston et al. (1985), Delage et al. (2012), Samarakoon et al. (2019), Maghsoodi et al. (2020), Samarakoon et al. (2022), Huancollo et al. (2023), among others, observed an increase in shear strength of NC clays after a heating and cooling cycle, consistent with the contraction and expansion reported by Campanella and Mitchell (1968) during heating and cooling. Samarakoon et al. (2022) found that normally consolidated clays with a greater initial effective stress associated with a greater depth in a soil profile will have a greater increase in undrained shear strength after heating. Huancollo et al. (2023) carried out thermal triaxial tests to assess the improvement of fine marine clay via thermal consolidation and recorded encouraging results in terms of undrained shear strength and stiffness. Samarakoon and McCartney (2023) and Samarakoon et al. (2022) also found that a heating-cooling cycle leads to a hardening effect on the small-strain shear modulus, with similar effects observed for fully drained heating and cooling and undrained heating and cooling followed by drainage after reaching a target temperature.

Britto et al. (1989) presented the results of an experimental study on thermal consolidation around a cylindrical heat source using physical models in a centrifuge. The findings were highly satisfactory when compared to those obtained with analytical solutions of the diffusion equation. Zeinali & Abdelaziz (2021) used the results from triaxial thermal tests to validate an analytical solution for evaluating pore pressure development and posterior volumetric strains of fine soils when subject to two rates of transient thermal loads. Using centrifuge modeling and a cylindrical heat source embedded in soil, Ghaaowd and McCartney (2018) found that pore water pressure begins to rise immediately after an increase in heat source temperature, even before the temperature increase reaches areas farther from the heat source. Ghaaowd et al. (2022) conducted experimental studies in a geotechnical centrifuge to evaluate the improvement in the pullout capacity of clayey soils after thermal consolidation, using a torpedo pile as a heat source. The results indicate a considerable improvement in pile pullout capacity after thermal consolidation. The zone of improvement was a question remaining from this study, and most improvement occurred in the soil near the pile interface.

There have been several studies who have performed analyses of thermal consolidation in saturated soils. Savvidou and Booker (1989) presented analytical results for the problem of consolidation around a point heat source in saturated soil. Savvidou and Booker (1991) later expanded this analytical solution to find an approximate solution for consolidation around a cylindrical heat source. Chaudhry et al. (2019) reviewed the analytical solution of Booker and Savvidou (1985) for heat diffusion problems from a point source embedded in a porous medium and reached different analytical solutions. This study was numerically verified by finite element analysis. Samarakoon and McCartney (2023) developed a coupled heat transfer and water flow model to study the thermal consolidation of normally consolidated soils surrounding a porous heat source and validated the model against data from the literature. Overall, these studies indicate that further experimental data from boundary value problems involving thermal consolidation is necessary for validation.

EXPERIMENTAL PROCEDURE

Model setup

A 500 mm-high cylindrical container with an internal diameter of 464mm was used to restrain the soil layer in the test (Figure 1). Three valves were installed in the container wall for drainage, two near the bottom and one near the top. A layer of highly permeable porous stone was laid on the floor of the container to allow drainage from both boundaries of the soil layer to accelerate soil consolidation. A 50mm of water level was maintained above the soil surface. To monitor pore water pressure dissipation during consolidation, pressure transducers (EPB-PW Miniature Pressure Transducer from TE Connectivity) were installed through the container wall at depths of 170, 290 and 410 mm from the top and denominated PP C1, PP C2 and PP C3, respectively. Two laser displacement sensors (Wenglor CP35MHT80) were also installed to monitor settlement of the top layer of soil inside the container during consolidation.

Heater (pile), instrumentation and temperature control

A 250 mm-long hollow aluminum torpedo pile was manufactured, with an external diameter of 19mm. A 180 mm long and 13 mm wide RAPID PAK 0301 electric heating element (750W) was installed inside the pile. A thermal paste from IMPLASTEC was used to facilitate heat transfer from the element to the pile body. Figure 2 shows a model of the torpedo pile and heating element used. It is clear from this figure that the tip of the energy pile is not thermally active, so heating is expected to occur mainly in the region of soil in the first 235 mm of the soil layer.

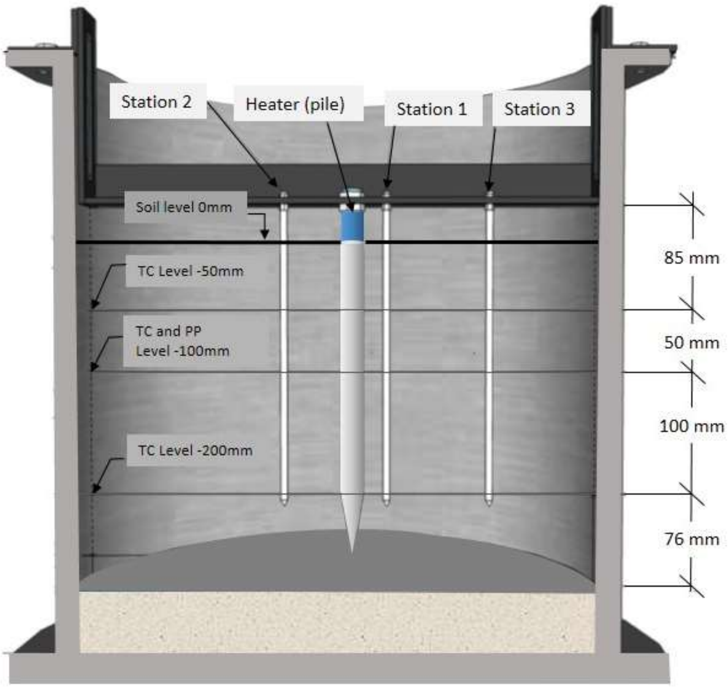

Figure 1 – Overall view of the test model and monitoring stations

Figure2. Torpedo pile and heating element

Three monitoring stations were installed at 30 (station 1), 60 (station 2) and 120mm (station 3) from the pile (heat source) to record temperature and pore water pressure distribution at specific points inside the soil. These distances are measured from the center of heater to the center of the station. Each station consists of a rod on which the thermocouples (TT-K-36-500, type K), however only station 1 and 2 had pore pressure transducers installed, as shown in Figure 3. Both the torpedo pile (hereafter referred to as the heater) and monitoring stations are coupled to a steel support bar attached to the top of the container. An insulating cap minimizes heat transfer from the heater to the steel support bar.

The three monitoring stations include thermocouples at depths of 50, 100 and 200 mm, respectively. Monitoring stations 1 and 2 also include pore water pressure transducers at a depth of 100 mm, corresponding to mid-height of the heated pile. The overall setup of each monitoring station is shown in Figure 3. Hereafter, each instrument will be identified according to the monitoring station where it is located, the type of instrument (TC for thermocouple and PP for pore water pressure transducer) and its installation depth. For example, the designation TC1.1 indicates a thermocouple on monitoring station 1 at a depth of 50 mm (depth 1), with PP identification following the same pattern. Three thermocouples were installed on the outer surface of the pile at the center of the heating element (100 mm) to provide feedback to the temperature control system, which consisted of a Watlow EZ-Zone controller that enables closed-loop temperature control. As the focus of this study was not on the mechanical penetration or pullout response of the torpedo pile, these sensors on the outside of the heater were deemed to be reasonable.

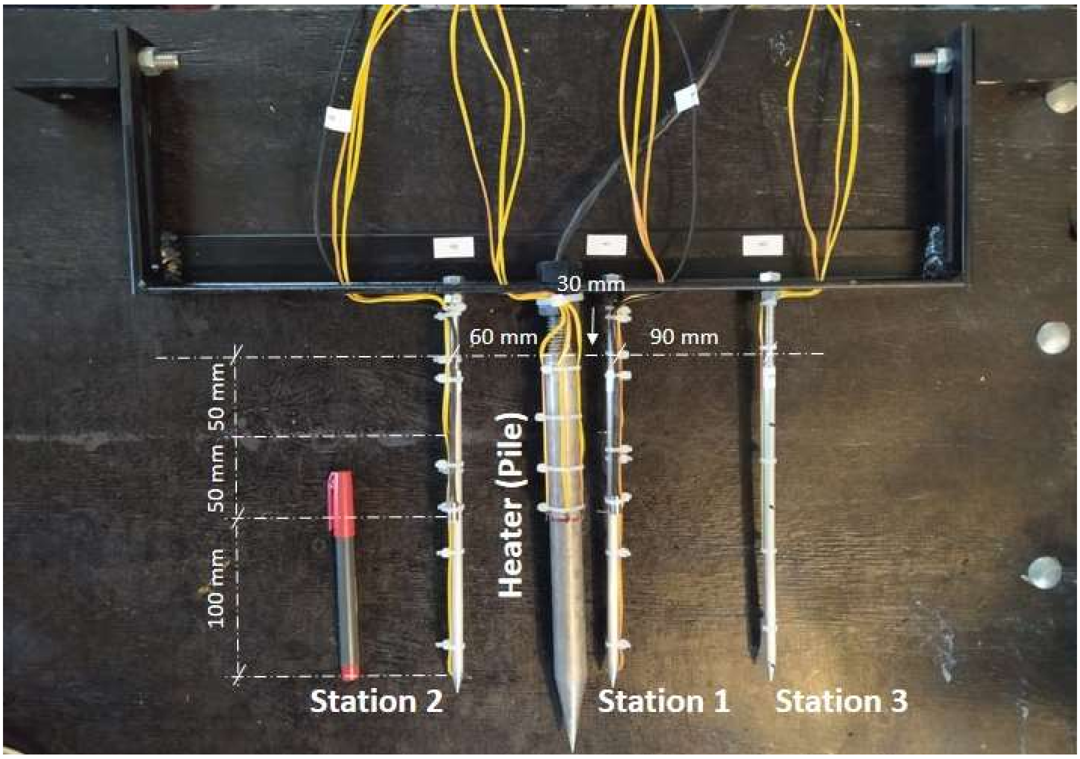

Figure 3. Position of the heater and monitoring stations used during thermal consolidation (L=200mm)

T-Bar penetration tests

To analyze the undrained shear strength profile at different distances from the heat source, a cross-shaped support structure was built for four simultaneous T-bar penetration tests conducted at distances of 4, 6, 8 and 16 times the heater radius (Figure 4). These tests aimed to assess the increase in soil shear strength in relation to distance from the heater and the resulting area affected by the temperature variation. The diameter and length of the T-bars were 7 and 14mm, respectively. The undrained shear strength profile was then calculated using the methodology proposed by Stewart and Randolph (1994). The penetration load was measured by a 50N SV-50 load cell (Alfa Instruments) installed at the top of the rod and the net load was measured by strain gauges on the shaft installed directly above the T-bar to eliminate the effect of friction from the shaft.

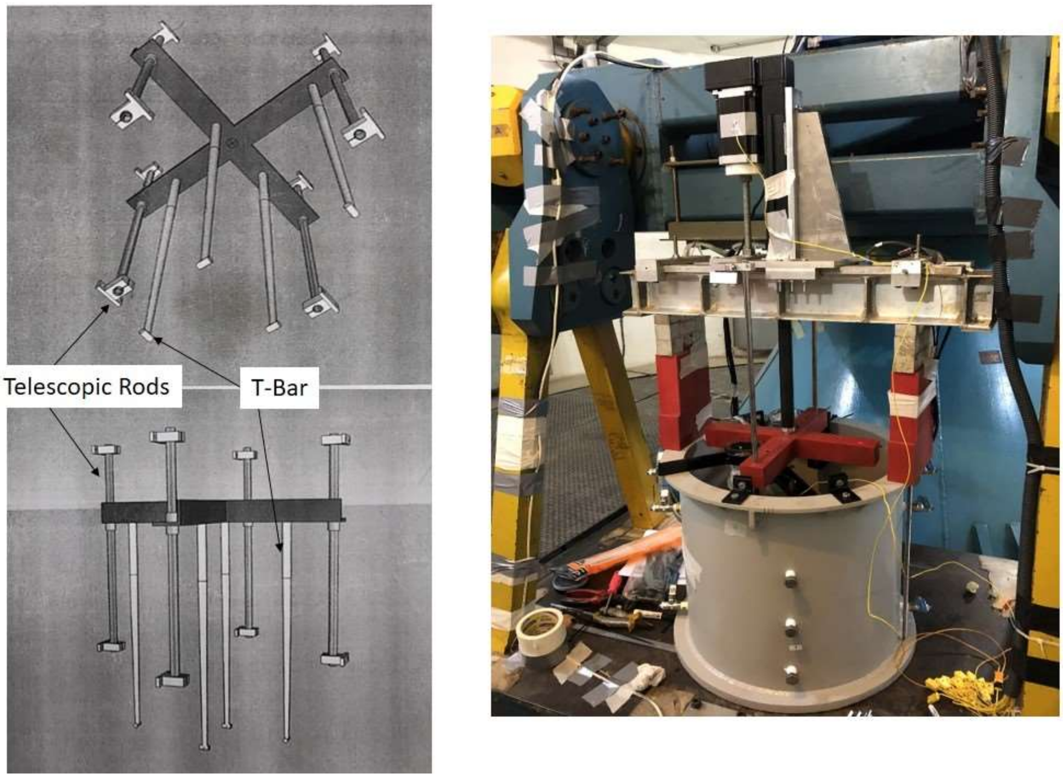

Figure 4. T-bar support structure and positioning of the T-bars and their installation in the centrifuge.

Slurry consolidation

The soil slurry used in the physical model was prepared from a mixture of kaolin (40%) and metakaolin (60%), whose characteristics are presented in Table 1.

Table 1. Slurry characterization

Liquid Limit	45.4%
Plastic Limit	26.5%
Plasticity Index	18.9%
Specific Gravity	2.64
Coefficient of Consolidation	7.2×10-3 cm2/s
USCS Classification	CL (low plastic clay)
Passing #200 sieve	100%

The slurry was prepared with an initial gravimetric water content corresponding to 1.5 times the liquid limit of the mixture. Initially, the slurry was homogenized in a mechanical mixer for 30 minutes, and then transferred to another adapted mixer with a vacuum inlet to extract moisture from the mixture. This procedure aims to keep the soil near or at saturated condition.

A benchmark large-scale consolidation test at 1g, was carried out in order to capture the compressibility characteristics of the mixture. The test was performed in the same container used in the centrifuge test and the one-dimensional curve can be seen in Figure 5. The normal compression line inclination (λ) was 0.193.

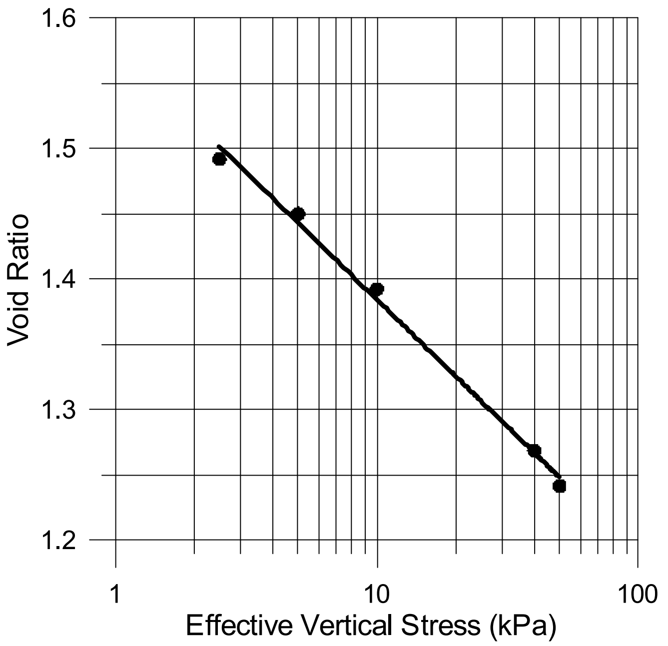

Figure 5 – One dimensional stress strain curve from large consolidation test

Consolidation for the centrifuge tests was performed, initially at 1g, inside the container in four soil layers, in a large consolidometer load frame installed in the laboratory. After slurry preparation, the target soil volume corresponding to each layer was placed in the cylindrical container (464 mm in diameter and 500 mm high). Each stage was designed to produce a 70 mm-thick layer after consolidation, under a load slightly higher than that applied during the centrifuge run to obtain a lightly overconsolidated (LOC) profile with an approximate overconsolidation ratio (OCR) of 2.5. The total thickness of the four layers to obtain the desired shear strength profile was 280mm, as shown in Figure 6. The final average void ratio after consolidation varied between 1.25 and 1.29, resulting in a degree of saturation of at least 97%. Table 2 includes a summary of the parameters before and after mechanical consolidation for the reference test, E1 as well as the heated tests E2 and E3.

Table 2. Data from soil layers during 1G consolidation. a) Test E1, b) Test E2 and c) Test E3.

a)

Layer	**Before mechanical consolidation**			**After mechanical consolidation**		
	e	**ρ (g/cm³)**	**w (%)**	**e**	**ρ (g/cm³)**	**w (%)**
Layer 1	1.81	1.58	67.5	1.45	1.66	53.9
Layer 2	1.83	1.57	68.3	1.25	1.72	46.0
Layer 3	1.85	1.57	69.2	1.18	1.74	43.7
Layer 4	1.85	1.55	67.0	1.14	1.73	40.3
Weighted mean	1.83	1.56	68.0			

b)

Layer	**Before mechanical consolidation**			**After mechanical consolidation**		
	e	**ρ (g/cm³)**	**w (%)**	**e**	**ρ (g/cm³)**	**w (%)**
Layer 1	1.76	1.60	67.7	1.48	1.67	57.2
Layer 2	1.84	1.57	69.1	1.32	1.70	49.6

Layer 3	1.81	1.58	68.1	1.21	1.74	45.5
Layer 4	1.80	1.59	68.8	1.16	1.76	44.6
Weighted mean	1.80	1.59	68.5			

c)

Layer	**Before mechanical consolidation**			**After mechanical consolidation**		
	e	**ρ (g/cm³)**	**w (%)**	**e**	**ρ (g/cm³)**	**w (%)**
Layer 1	1.76	1.61	68.3	1.43	1.69	55.6
Layer 2	1.86	1.56	69.0	1.36	1.68	49.8
Layer 3	1.77	1.60	67.2	1.16	1.76	44.2
Layer 4	1.81	1.59	68.9	1.16	1.76	44.1
Weighted mean	1.80	1.59	68.4			

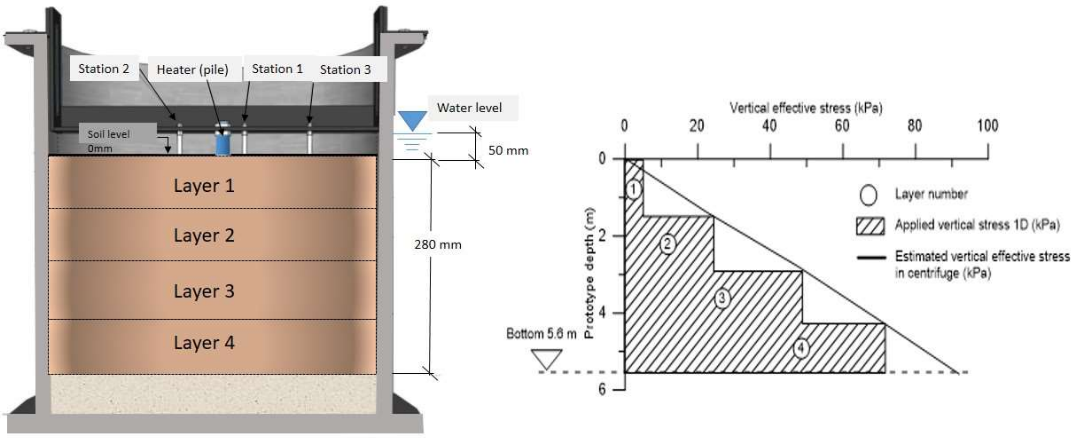

Figure 6. Consolidation scheme at 1G prior to centrifugation

After consolidation at 1G, the assembly consisting of the heater (pile) and monitoring station rods with instruments was carefully embedded in the soil inside the container. After embedding the assembly vertically within the soil layer, the resulting pore pressures were allowed to stabilize. The support structure with the T-bars hanging above the soil layer was then positioned to begin the centrifuge tests.

Centrifuge tests

Three tests were carried out in a geotechnical centrifuge, one with no heating (test E1) and two in which the pile was heated at 65 and 45°C and cooled afterwards (tests E2 and E3, respectively). The different stages of the geotechnical centrifuge tests are described in Table 3.

Table 3 –Stages followed for the centrifuge tests

Test stage	**Description**	**Environment**
1	Soil preparation and mechanical consolidation in 4 layers	Outside centrifuge
2	Installation of the pile and instrumented stations	
3	Self-weight consolidation at 20g	
4	Heating the torpedo pile	During centrifugation
5	Cooling the torpedo pile	

There was no heating or cooling in the reference test E1, as its objective was to determine the soil shear strength profile before thermal treatment and use these results as reference for the remaining tests. To ensure similarity between the tests, the reference test was run with the pile and instrumented rods embedded in the model, as in the heating tests.

When a gravitational field of 20g was reached, increases in pore water pressure were observed in the transducers on the container walls and the monitoring station rods. At this point, the pore pressure was allowed to dissipate, which took an average of three hours. Immediately after consolidation was completed, the T-bar drive system was activated at a speed of 20mm/s, embedding the T-bars to a planned depth of 280mm. This reference test was conducted at an average room temperature of 26.8°C, which was relatively constant during testing due to the use of an air circulation system.

Tests E2 and E3 consisted of thermal treatment at maximum temperatures of 65 and 45°C, respectively, immediately after mechanical consolidation. Once the desired temperature was reached in tests E2 and E3, it was maintained until stabilization of the sensors readings located in the three instrumented rods. This stage lasted approximately 4h40min. Next, the heating was switched off to allow the soil to return to room temperature naturally (uncontrolled), which took around 2 hours in both tests. After the soil heating and cooling cycle, the T-bar tests were initiated at a penetration speed of 20 mm/s, where undrained behavior is assumed to occur in accordance with Finnie and Randolph (1994) and Stewart and Randolph (1994).

RESULTS

Reference Test E1

The undrained shear strength profile obtained from the T-bars in test E1 are shown in Figure 7. The undrained strength profiles of T-bars 3 and 4 (at distances of 4 and 8 times the pile diameter, respectively) are slightly lower than those of T-bars 1 and 2 (located at 2 and 3 times the pile diameter). This is because the soil closer to the container wall experiences boundary effects and is, therefore, less consolidated than zones further from the wall. It is important to note that although the profile increases with depth, it is relatively constant in the layers created during consolidation at 1g. In the case of undrained strength, the void ratios in each layer were relatively constant, generating localized overconsolidation in each layer. As such, for overall assessment, an intermediate mean undrained shear strength profile was established between the undrained shear strength profiles at different radial distances, depicted by the red line in Figure 7.

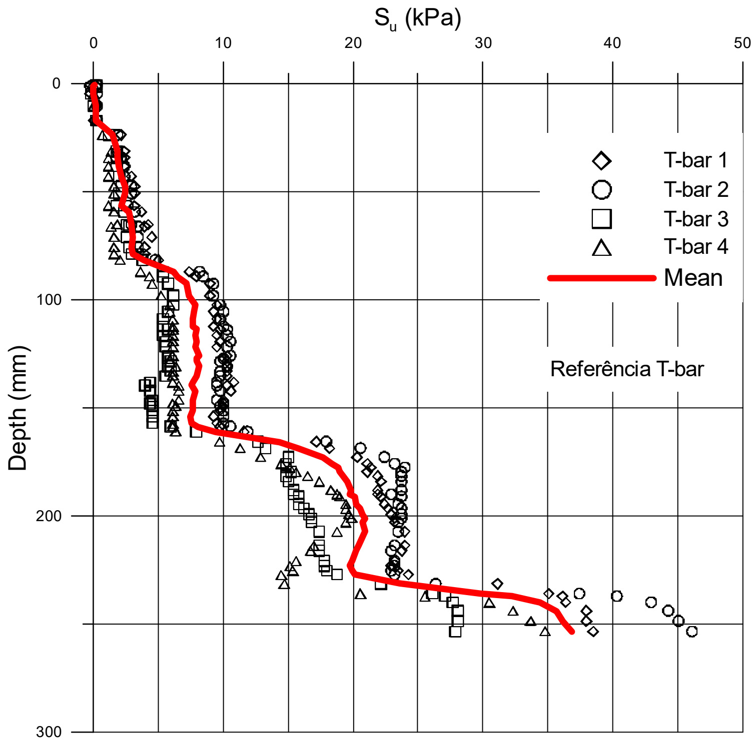

Figure 7. Undrained shear strength profiles for reference test E1

Thermal Consolidation Phase

Once the desired centrifuge acceleration was reached, the excess pore pressures generated during mechanical consolidation in the centrifuge were allowed to stabilize and the heating cycle then initiated in the pile, up to maximum temperatures of 65 and 45 °C, for tests E2 and E3, respectively. The temperature increases applied to the heater in relation to the temperature in test E1 were 38.2 and 18.2°C for tests E2 and E3, respectively. The responses of the sensors installed in the monitoring station rods are presented in Figure 8 where the temperatures are plotted as a function of normalized radius distance for tests E2 and E3.

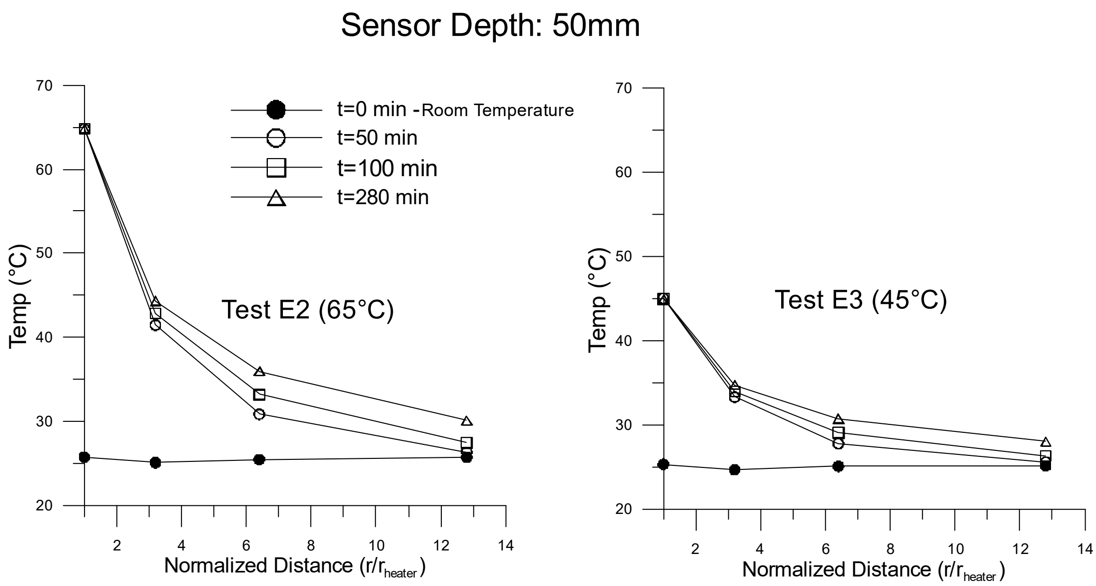

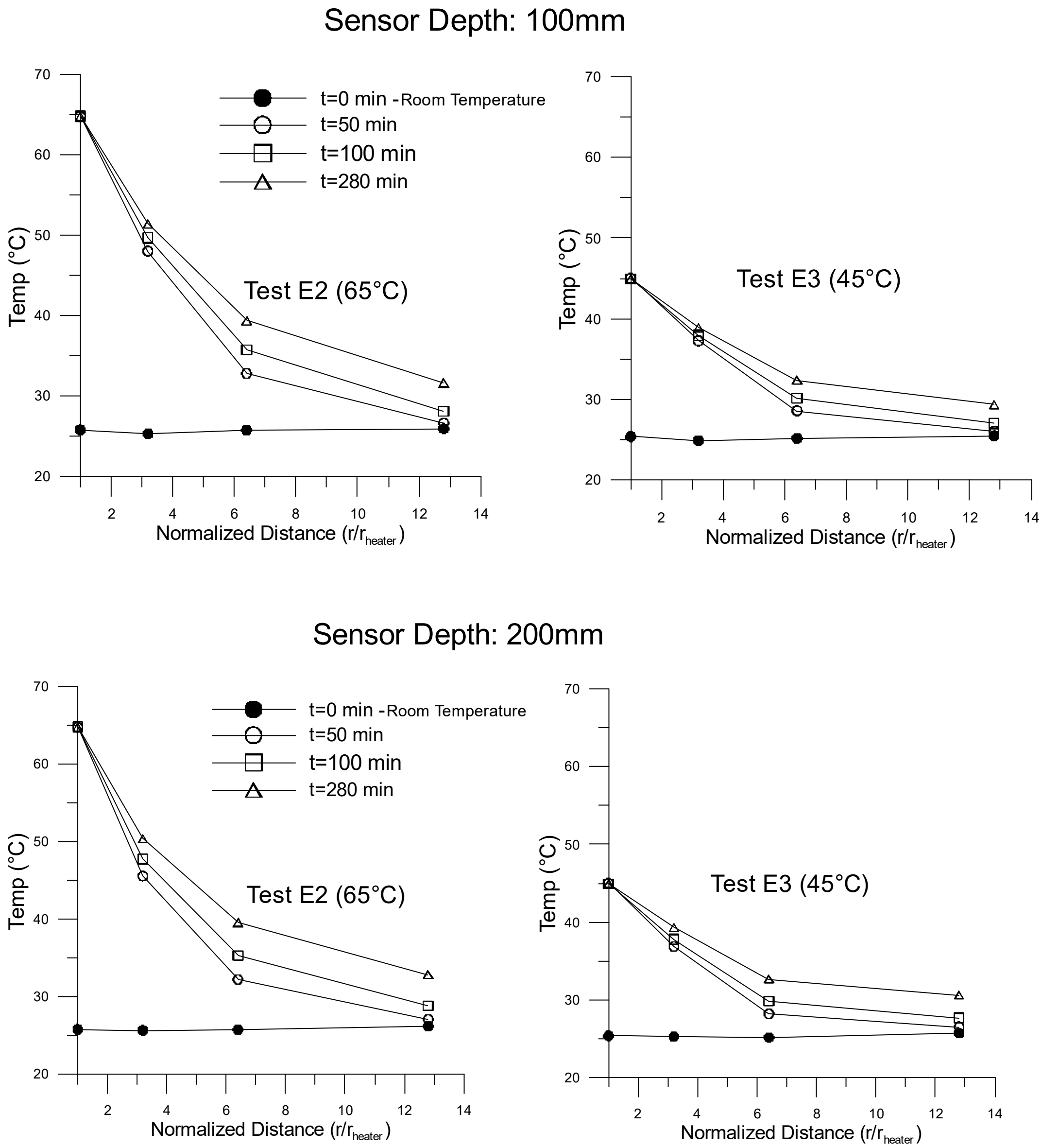

Figure 8. Temperature distributions during heating

The spatial temperature variation exhibited exponential trend behavior as a function of normalized distance, which is consistent with the theory of infinite line heat source solution as shown by Britto et al (1989). Thus, it is apparent that the temperature increase was greater between the middle (100 mm) and base of the heater (200 mm) in both tests. Cooling occurred naturally by switching off the heater. Regardless of the maximum temperature reached, the average time elapsed to return to room temperature was approximately 2h10min.

The temperature increase and subsequent cooling generate excess pore water pressure that subsequently dissipates, as observed in Figure 9 at the 100 mm-deep monitored points at normalized distances of (r/r_{heater}) of 3.2 and 6.3. Pore water pressure peaks suddenly during heating and then declines, confirming slight overconsolidation due to prior consolidation of the layers at 1g environment, as previously mentioned. Pore water pressure increases during cooling, albeit without returning to initial values.

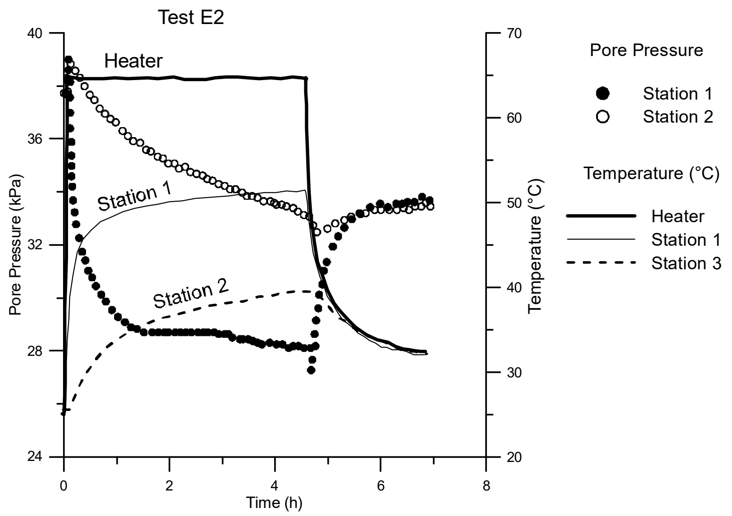

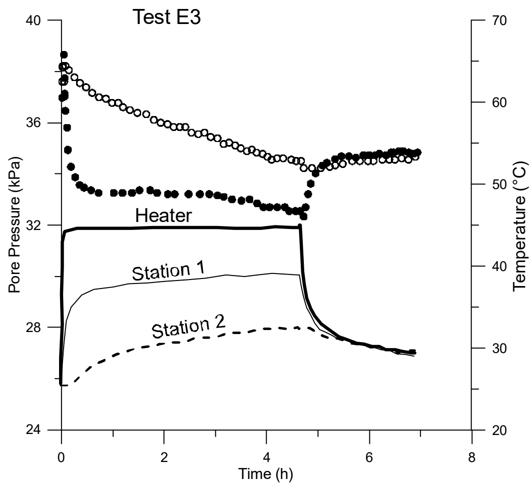

Figure 9 – Pore water pressure variation during heating and cooling for the tests E2 and E3.

Despite the rapid temperature increase in the heater, the measurements at stations 1 and 2 presented different heating patterns. As the heater temperature reaches its maximum in both testes (65 and45°C) almost immediately, the temperatures recorded by the two stations follow an exponential-like trajectory, with, after long term, very low rate about 0.003°C/min, which, according to Morteza Zeinali & Abdelaziz, (2021) allows the dissipation of the pore pressure during heating process. The measurements at station 1 presents an initial heating increase rate higher than of station 2, however, after 2 hours they show similar rates. The initial rate of station 1 was about 0.5°C/min while the measurements at station 2 showed an initial rate of 0.033°C/min. The rate of pore pressure dissipation was decreasing for station 1 after approximately 2 hours, while station 2 was still in a clear process of quasi-static dissipation. It is interesting to note that in test E2, the heater temperature reached 65°C and the measurements at station 1 tended to stabilize around 53°C. On the other hand, the test E3, where the heater temperature was 45°C, the temperature in station 1 tends to stabilize at 40°C. When the pore pressure drops quite rapidly at the location of station 1, water flow occurs from station 2 towards station 1 due to the difference in total head. During the cooling phase, both stations recorded similar recovery patterns.

As stated, the T-bars tests were carried out simultaneously at distances 2, 3, 4, and 8d from the heat source, where d is the pile (heater) diameter. The results are shown in Figures 10 along with the mean of the reference T-bar measurements. To compare the reference and thermal treatment results, the increase in strength was calculated point by point via statistical analysis, disregarding the first 15 mm from the top, an area affected by the consolidation cap at 1g. With a view to reducing the influence of undrained strength fluctuations across the soil profile, the mean of the four T-bars in E1 (red circles in Figure 10) was used as reference for comparison with E2 and E3. As such, the results of each T-bar in E2 and E3 were compared with the mean profile of the reference T-bars. The improvement results are defined as the simple quotient of the individual strength values of each T-bar in relation to the strength measured at the same corresponding depth of the mean curve of the reference T-bars. It is important to note the pattern of an increase in temperature in the container as a function of sensor distance and their respective depths, as observed in Figure 8. Heat propagation is greater at the location of the 100 mm-deep sensor in monitoring station 1 in both experiments. Heat concentration is less evident at station 2 and greater at station 3 for a depth of 200 mm.

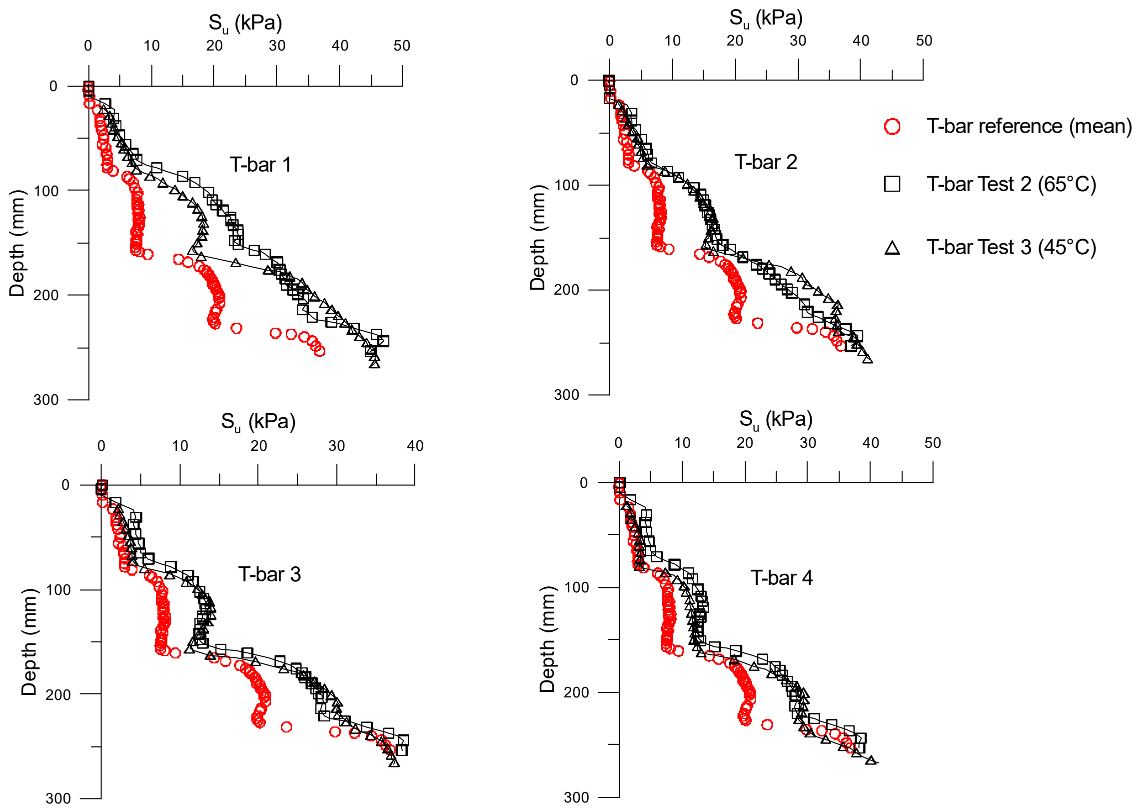

Figure 10. Undrained shear strength before and after thermal consolidation.

DISCUSSION

Undrained Shear Strength after Thermal Consolidation

The S_u profile for the reference tests showed that the soil layers were very well-defined, with clear strength plateaus between them. Thus, to enable direct comparison of undrained strength values between tests, the four soil layers were compared individually, calculating the mean of the strength values obtained for the T-bars in E2 and E3 and the mean of E1 results in the respective layers (Figure 11). However, it was found valuable to include the overall mean of the strength ratio, which is calculated using the mean of the four T-bars for each layer.

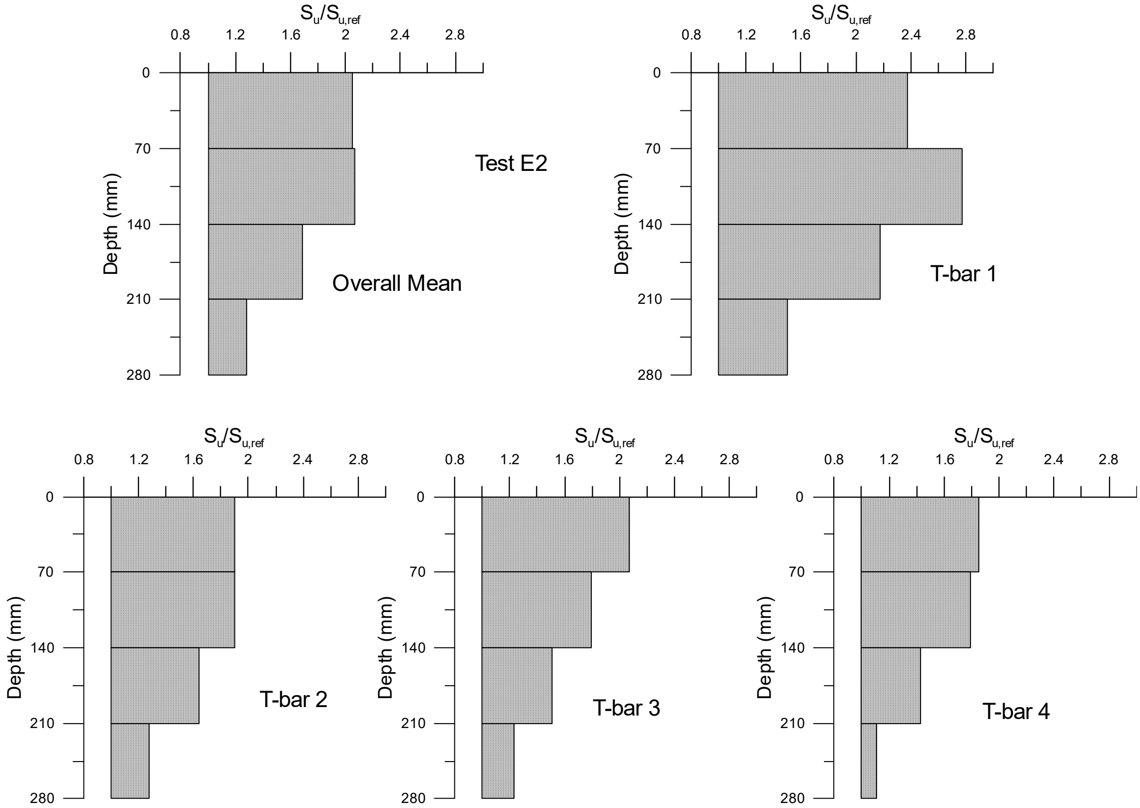

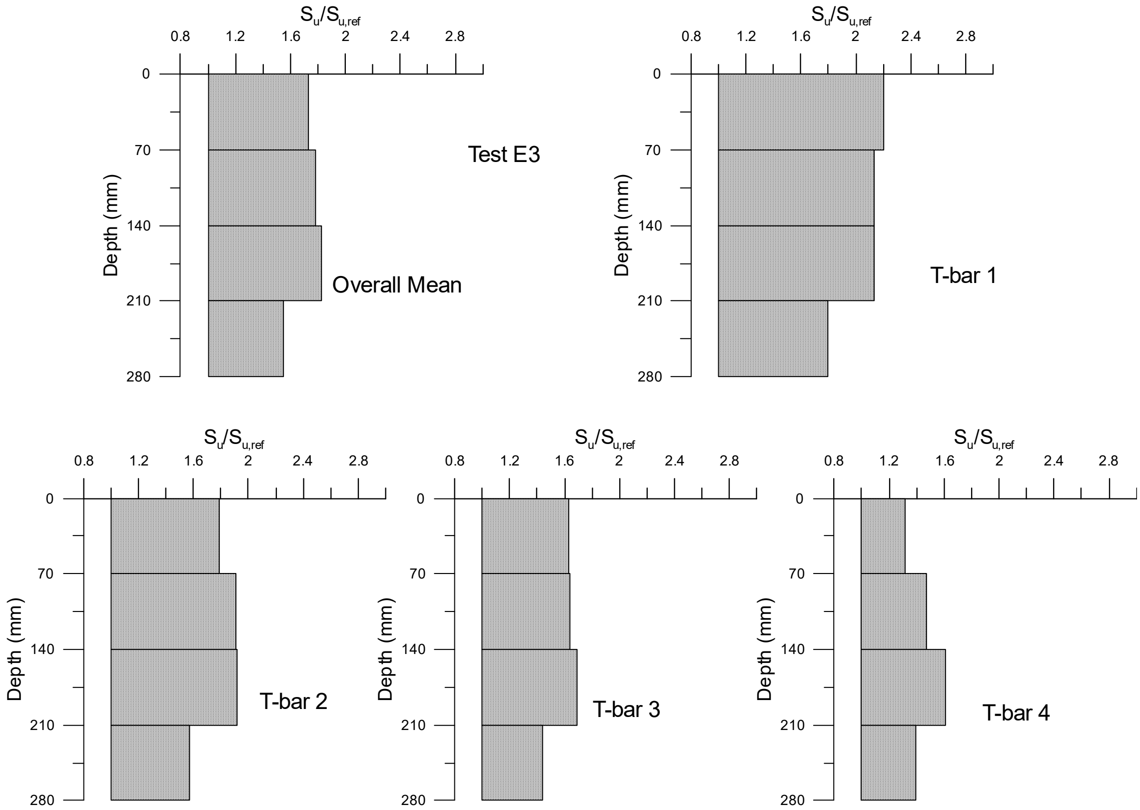

Figure 11. Gain in normalized undrained shear strength with model depth and distance from the heat source.

For T-bars 1 to 4 in E2, heated to 65°C and then cooled to room temperature, the results indicate significant undrained shear strength gains at all locations. Increases were more evident for T-bar 1, with the gain in the second layer reaching around 2.6 times the reference undrained shear strength value. More modest gains were observed in the layer between depths of 210 and 280 mm for all the T bars, an area farther from the direct influence of heating. For T-bar 1, as observed in test E3, increases were greater in the second layer, at approximately 2.2 times the reference undrained strength. Strength gains in the first soil layer were low for the remaining T-bars. This is because heat transfer in areas near the surface occurs primarily by convection, which is affected by the propagation time and surface exposure to wind effects during the centrifuge flight. Analysis of the complete undrained strength profile with depth indicated that the results obtained in test E3 (heating up to 45°C) were similar to those of E2. However, comparison of the mean of each layer of the reference test showed more modest, albeit still significant, gains in relation to test E2.

In order to analyze the whole set of points where undrained shear strength was measured along with depth, three classes for indicating the amount of improvement were created: Very high improvement, where the undrained shear strength gain is higher than 3.0; High improvement, where the gain is between 2.0 and 3.0, and moderate improvement, where the gain is higher than 1.0 and lower that 2.0 .

Figure 12 shows a direct comparison from point to point for T-bars 1 to 4 of tests E2 and E3 with the mean S_u from reference test at same corresponding depth. In T-bar1 of the test E2, that is close to the heat source up to depth 170mm, very high gain has been observed, For the T-bar tests located far from the heat source, T-bar 3 and 4, the gain was more modest, but still quite higher as compared to the reference test. It is interesting to note that the highest gain for the test E2, are located between the depth of 0 and 170mm, which coincides with the length of the heating element inside the pile. Below this depth, the gain was moderate.

Considering the test E3, no gain fell into "very high improvement" category. However, for T-bar1 and T-bar2, the gain was in the limit between the two categories. As observed in test E2, the T-bar1 of the test E3 also shows the highest gain, however with less intensity. Some very few points showed values less than 1 in the tip of the heater. This is attributed to the natural variability of the soil that is not impacted by the thermal consolidation, deeper than 240mm.

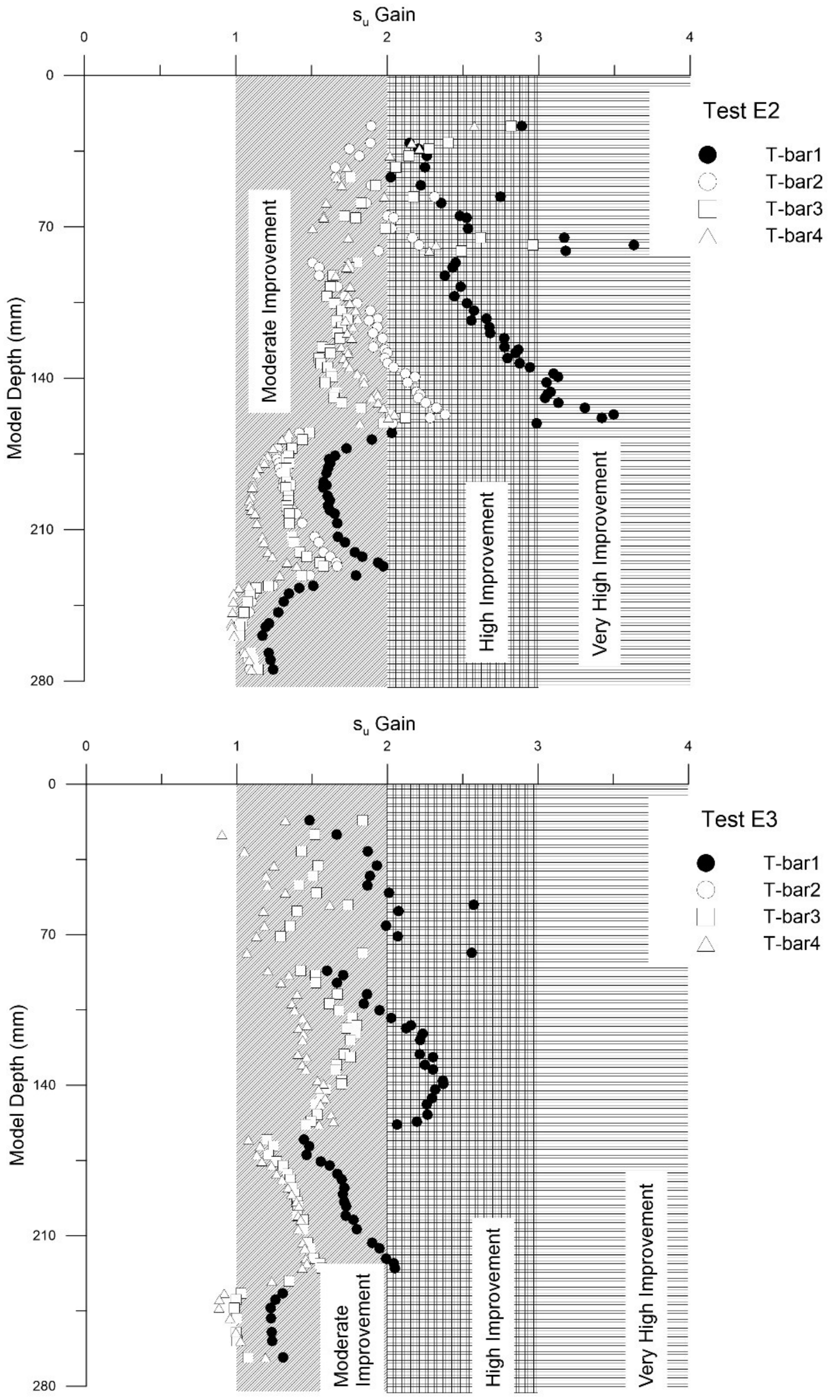

Figure 12. Gain in undrained strength for the whole set of values from each T-bar after thermal treatment compared to the mean values from the reference test.

As such, strength gains are larger for higher temperature increases due to the greater impact on pore water pressure generated during heating.

To give an overall and straight impression of the gain of undrained strength for both Tests E2 and E3 along the whole volume of soil impacted by the temperature, the mean of each T-bar was divided by the mean of the reference T-bar (Test E1) and plotted against the distance from the heat source (Figure 13) for all values. Despite the large variation, the tendency of the gain in undrained shear strength is clear.

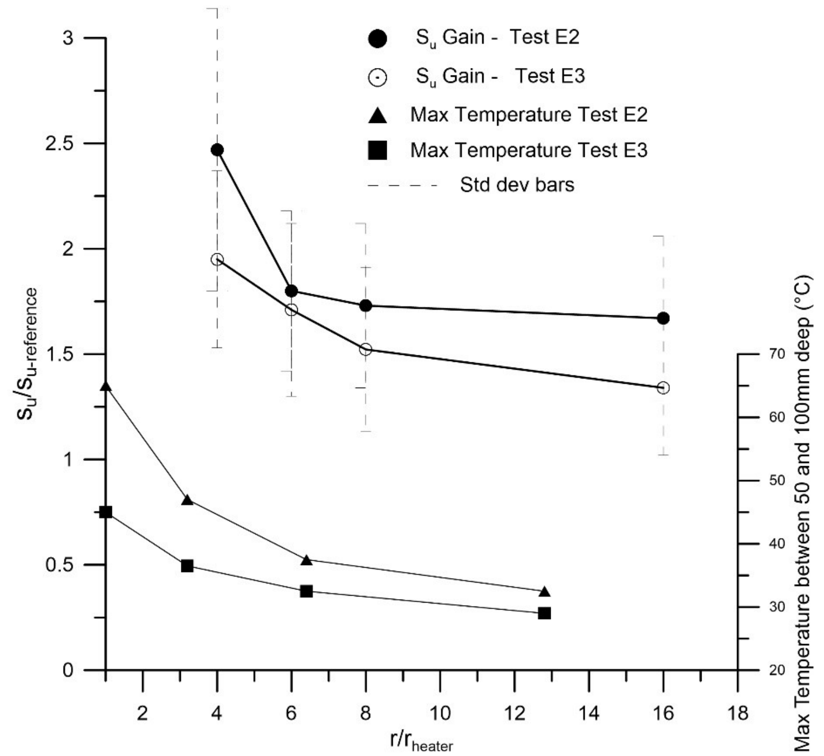

Figure 13. Overall undrained shear strength gain as a function of the distance from the heat source and the maximum reached temperature for tests E2 and E3.

Considerable gains in undrained strength with radius distance from the heat source, is associated with induced flow due to difference in total head caused by locally pore pressure generation after heating. This has promoted additional consolidation, which can reach distances farther than 16 times the heated pile radius, where the undrained strength increase reaches up to 50%. It is interesting to mention that the curves representing the gain of undrained shear strength follow the same shape of the temperature distribution during heating as shown in Figure 8. This feature is particularly interesting for considering pile group arrangement where the heat source is placed at the center of the group, improving all the adjacent piles. Remarkable improvement is seen in regions close to the heat source, which are directly responsible for the ultimate capacity of this kind of anchorage, working mainly under pull out loads.

CONCLUSION

The effect of thermal induction on volume change and the resulting shear strength gain in normally or lightly overconsolidated cohesive soils has been more widely studied in recent years. However, physical modeling has been evidenced to be a practical and efficient technique, particularly in environments inhospitable to humans where traditional soft soil improvements are not feasible. This study used geotechnical centrifuge modeling to evaluate the effectiveness of thermal soil consolidation and the resulting shear strength gain with depth (stress level), heating intensity and distance from the heat source. This technique was proposed to investigate its use in marine anchoring systems, with the additional goal of emitting heat to promote consolidation in the surrounding area and enable verticalization of the load, thus reducing the number of mooring lines and congestion in the drilling and exploration area. The results were promising, with shear strength gains of up to 220% in the areas closest to the pile, which is also a heat source. Using the pile itself as a heater source needs further technological development, and it is out of the scope of this study, however, the amount of soil improved by the heating, shown in the tests, confirm the efficiency of the method. The effects of the improvement, albeit smaller, can be felt at distances up to 16 times greater than the radius of the source, indicating that for a cluster or group of piles, a single equidistant heat source can be highly effective for the whole set of pile composing the group, given the radial heat conduction.

ACKNOWLEDGEMENT

The Authors are grateful to the Brazilian Oil Company – Petrobras for supporting this research through the Grant No 0050.0098204.15.9

REFERENCES

Abuel-Naga, H. M., D. T. Bergado, A. Bouazza, M. Pender, G. V. Ramana, Zoheir Bellia, Moulay Smaine Ghembaza, et al. 2007. "Volume Change Behaviour of Saturated Clays under Drained Heating Conditions: Experimental Results and Constitutive Modeling H.M." *Computers and Geotechnics* 30 (13): 1303–36. https://doi.org/10.1002/nag.

Abuel-Naga, H. M., D. T. Bergado, A. Bouazza, and G. V. Ramana. 2007. "Volume Change Behaviour of Saturated Clays under Drained Heating Conditions: Experimental Results and Constitutive Modeling." *Canadian Geotechnical Journal* 44 (8): 942–56. https://doi.org/10.1139/T07-031.

Booker, J R, and C Savvidou. 1985. "Consolidation around a Point Heat Source." *International Journal for Numerical and Analytical Methods in Geomechanics* 9 (2): 173–84. https://doi.org/https://doi.org/10.1002/nag.1610090206.

Britto, A.M., C. Savvidou, D.V. Maddocks, M.J. Gunn, and J. R. Booker. 1989. "Numerical and Centrifuge Modelling of Coupled Heat Flow and Consolidation around Hot Cylinders Buried in Clay." *Geotechnique* 39 (1): 13–25. https://doi.org/https://doi.org/10.1680/geot.1989.39.1.13.

Campanella, Richard, and James Mitchell. 1968. "Influence of Temperature Variations on Soil Behavior." *Journal of the Soil Mechanics and Foundations Division* 94 (3): 609–734.

Chaudhry, Aqeel Afzal, Jörg Buchwald, Olaf Kolditz, and Thomas Nagel. 2019. "Consolidation around a Point Heat Source (Correction and Verification)." *International Journal for Numerical and Analytical Methods in Geomechanics* 43 (18): 2743–51. https://doi.org/10.1002/nag.2998.

Delage, P., N. Sultan, and Y. J. Cui. 2012. "On the Thermal Consolidation of Boom Clay." *Canadian Geotechnical Journal* 37 (2): 343–54. https://doi.org/10.1139/t99-105.

Finnie, I.M.S., and M. F. Randolph. 1994. "Punch-through and Liquefaction Induced Failure of Shallow Foundations on Calcareous Sediments." In *Proceedings of the International Conference on Behaviour of Offshore Structures, BOSS'94*, 217–30.

Ghaaowd, I., J.S. McCartney, and F. Saboya. 2022. "Centrifuge Modeling of Temperature Effects on the Pullout Capacity of Torpedo Piles in Soft Clay." *Soils and Rocks* 45 (1). https://doi.org/10.28927/SR.2022.000822.

Ghaaowd, Ismaail, Atsushi Takai, Takeshi Katsumi, and John S. McCartney. 2015. "Pore Water Pressure Prediction for Undrained Heating of Soils." *Environmental Geotechnics* 4 (2): 70–78. https://doi.org/10.1680/jenge.15.00041.

Ghaawod, Ismaail, and John S. McCartney. 2018. "Centrifuge Modeling of Temperature Effects on the Pullout Capacity of Energy Piles in Clay." *Proceedings of the 43rd Annual Conference on Deep Foundations*, 24–27.

Han, Congcong, and Jun Liu. 2020. "A Review on the Entire Installation Process of Dynamically

Installed Anchors." *Ocean Engineering* 202 (March): 107173. https://doi.org/10.1016/j.oceaneng.2020.107173.

Houston, Sandra L., William N. Houston, and Neil D. Williams. 1985. "Thermo-Mechanical Behavior of Seafloor Sediments." *Journal of Geotechnical Engineering* 111 (11): 1249–63. https://doi.org/10.1061/(ASCE)0733-9410(1985)111:11(1249).

Huancollo, Hiden Jaime Machaca, Fernando Saboya Jr, Sergio Tibana, John Scott McCartney, and Ricardo Garske Borges. 2023. "Thermal Triaxial Tests to Evaluate Improvement of Soft Marine Clay through Thermal Consolidation." *GEOTECHNICAL TESTING JOURNAL* 46 (3): 579–97. https://doi.org/10.1520/GTJ20220154.

Keerthi Raaj, S., Nilanjan Saha, and R. Sundaravadivelu. 2023. "Exploration of Deep-Water Torpedo Anchors - A Review." *Ocean Engineering* 270 (June 2022): 113607. https://doi.org/10.1016/j.oceaneng.2022.113607.

Lauria, A., P. Loprieno, A. Francone, E. Leone, and G. R. Tomasicchio. 2024. "Recent Advances in Understanding the Dynamic Characterization of Floating Offshore Wind Turbines." *Ocean Engineering* 307 (May): 118189. https://doi.org/10.1016/j.oceaneng.2024.118189.

Maghsoodi, Soheib, Olivier Cuisinier, and Farimah Masrouri. 2020. "Thermal Effects on Mechanical Behaviour of Soil–Structure Interface." *Canadian Geotechnical Journal* 57 (1). https://doi.org/10.1139/cgj-2018-0583.

Morteza Zeinali, Seyed, and Sherif L. Abdelaziz. 2021. "Thermal Consolidation Theory." *Journal of Geotechnical and Geoenvironmental Engineering* 147 (1). https://doi.org/10.1061/(ASCE)GT.1943-5606.0002423.

Rui, Shengjie, Zefeng Zhou, Zhen Gao, Hans Petter Jostad, Lizhong Wang, Hang Xu, and Zhen Guo. 2024. "A Review on Mooring Lines and Anchors of Floating Marine Structures." *Renewable and Sustainable Energy Reviews* 199 (December 2023): 114547. https://doi.org/10.1016/j.rser.2024.114547.

Samarakoon, Radhavi A., Isaac L. Kreitzer, and John S. McCartney. 2022. "Impact of Initial Effective Stress on the Thermo-Mechanical Behavior of Normally Consolidated Clay." *Geomechanics for Energy and the Environment* 32: 100407. https://doi.org/10.1016/j.gete.2022.100407.

Samarakoon, Radhavi A., and John S. McCartney. 2023. "Simulation of Thermal Drains Using a New Constitutive Model for Thermal Volume Change of Normally Consolidated Clays." *Computers and Geotechnics* 153 (July 2022): 105100. https://doi.org/10.1016/j.compgeo.2022.105100.

Samarakoon, Radhavi, Ismaail Ghaaowd, and John S. McCartney. 2019. "Impact of Drained Heating and Cooling on Undrained Shear Strength of Normally Consolidated Clay." *Springer Series in Geomechanics and Geoengineering* 0 (217729): 243–49. https://doi.org/10.1007/978-3-319-99670-7_31.

Savvidou, C., and J. R. Booker. 1989. "Consolidation around a Heat Source Buried Deep in a Porous Thermoelastic Medium Woth Anisotropic Flow Properties." *International Journal for Numerical and Analytical Methods in Geomechanics* 13: 75–90.

SAVVIDOU, C, and J R BOOKER. 1991. "CONSOLIDATION AROUND A HEAT-SOURCE BURIED AT A FINITE DEPTH BELOW THE SURFACE OF A DEEP CLAY STRATUM." In *COMPUTER METHODS AND ADVANCES IN GEOMECHANICS, VOL 2*, edited by G BEER, J R BOOKER, and J P CARTER, 1085–89.

Stewart, D. P., and M. F. Randolph. 1994. "T-Bar Penetration Testing in Soft Clay." *Journal of Geotechnical and Geoenvironmental Engineering* 120 (12): 2230–35. https://doi.org/10.1061/(ASCE)0733-9410(1994)120:12(2230).

Trani, Laricar Dominic O., Dennes T. Bergado, and Hossam M. Abuel-Naga. 2008. "Thermal Effects on Undrained Shear Strength of Normally Consolidated Soft Bangkok Clay" 40972 (April 2015): 1069–76. https://doi.org/10.1061/40972(311)134.